

# Determining the accuracy of spatial gradient sensing using statistical mechanics

Bo Hu, Wen Chen, Wouter-Jan Rappel and Herbert Levine<sup>1</sup>

<sup>1</sup> *Department of Physics and Center for Theoretical Biological Physics,  
University of California, San Diego, La Jolla, CA 92093-0374*

(Dated: April 2, 2024)

Many eukaryotic cells are able to sense chemical gradients by directly measuring spatial concentration differences. The precision of such gradient sensing is limited by fluctuations in the binding of diffusing particles to specific receptors on the cell surface. Here, we explore the physical limits of the spatial sensing mechanism by modeling the chemotactic cell as an Ising spin chain subject to a spatially varying field. This allows us to derive the *maximum likelihood estimators* of the gradient parameters as well as explicit expressions for their asymptotic uncertainties. The accuracy increases with the cell's size and our results demonstrate that this accuracy be further increased by introducing a non-zero cooperativity between neighboring receptors. Thus, consistent with recent experimental data, it is possible for small bacteria to perform spatial measurements of gradients.

PACS numbers: 02.50.Le, 05.65.+b, 87.23.Ge, 87.23.Kg

Cells often direct their motion under the guidance of chemical gradients. This is essential for critical biological functions including neuronal development, wound repair and cancer spreading [1, 2]. To detect gradients, small organisms like bacterial cells usually employ a temporal sensing strategy by measuring and comparing concentration signals over time along their swimming tracks [3–6]. In contrast, eukaryotic cells are sufficiently large to implement a spatial sensing mechanism, as they can measure the concentration differences across their cell bodies. Measurements for both strategies are accomplished by specific cell-surface receptors which diffusing chemical particles (ligands) can bind to. Spatial sensing among eukaryotes exhibits a remarkable sensitivity to gradients of merely 1-2% across the cell [7–9]. Given the dynamic fluctuations in ligand-receptor interaction, the receptor signal is inherently noisy, as demonstrated by single-cell imaging experiments [10, 11]. This naturally raises a question concerning the reliability of spatial gradient sensing.

In analyzing bacterial chemotaxis, Berg and Purcell showed that the minimal uncertainty of mean concentration measurements is set by the diffusion of ligand particles [12]. This work has been extended to include ligand-receptor binding effects and possible receptor cooperativity [13–17]. The spatial sensing program concerns the acquisition of information regarding the asymmetry in space (the gradient steepness and direction). The accuracy of gradient measurements should similarly be limited by physical laws governing diffusion and stochastic ligand-receptor dynamics. There have been some studies on the limits to spatial sensing, but either for idealized sensing mechanisms that ignore the receptor kinetics [16] or based on specific transduction models [18]. In this Letter, we address this problem in a general way using a statistical mechanical approach where we view the surface receptors as a (possibly coupled) spin chain and treat the chemical gradient as a perturbation field. By calculating the system's partition function, we are able to derive the physical limits of gradient sensing for both indepen-

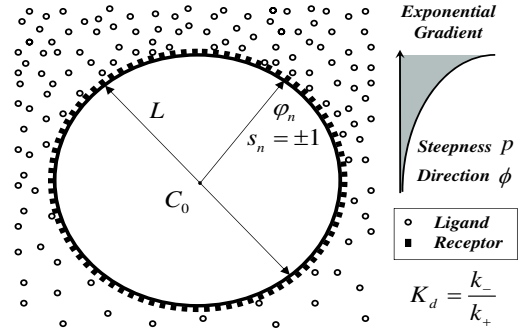


FIG. 1: Schematic representation of our model: a circular cell, covered with receptors, is placed in an exponential gradient. The forward and backward rates  $k_{\pm}$  control the transition between the bound and unbound states for the receptors.

dent receptors and for receptors exhibiting cooperativity. These limits allows us to predict that the strategy of spatial sensing may not be exclusive to large eukaryotic cells but may also be applicable to some bacterial cells [19], especially with the aid of receptor cooperativity.

We consider a circular cell with diameter  $L$  immersed in a chemoattractant gradient (Fig. 1). We suppose that there are  $N$  receptors distributed at equally spaced intervals on the cell's perimeter [20]. The angular coordinates of these receptors are indicated by  $\varphi_n = 2\pi n/N$  for  $n = 1, \dots, N$ . For analytical convenience, we assume that the gradient field takes an exponential profile, as was recently realized in experiments utilizing the social amoeba *Dictyostelium* [9, 21]. The local concentration at the  $n$ -th receptor is  $C_n = C_0 \exp[\frac{p}{2} \cos(\varphi_n - \phi)]$ , where  $C_0$  is the background concentration,  $p \equiv \frac{L}{C_0} \frac{dC}{dr}$  denotes the gradient steepness, and  $\phi$  indicates the gradient direction. Like a spin in physics, each receptor switches between two states: either active ( $s_n = +1$ ) or inactive ( $-1$ ). For independent receptors, a receptor is activated only if it is bound by ligand and inactive otherwise. Let the energy associated with the state  $s_n = +1$  (or  $-1$ ) be  $-\varepsilon_n$  (or

$+\varepsilon_n$ ) in units of the thermal energy  $k_B T$ . Then the “on” probability of the  $n$ -th spin is given by the Boltzmann distribution:  $P_{on} = e^{\varepsilon_n} / (e^{\varepsilon_n} + e^{-\varepsilon_n})$ . For simple receptor-ligand kinetics (Fig. 1), we have  $P_{on} = C_n / (C_n + K_d)$  in chemical equilibrium where  $K_d = k_- / k_+$  is the dissociation constant. Therefore, the free energy has the expression:

$$\varepsilon_n = \frac{1}{2} \ln \frac{C_n}{K_d} = \frac{1}{2} \ln \frac{C_0}{K_d} + \frac{p}{4} \cos(\varphi_n - \phi) \equiv \alpha_0 + h_n. \quad (1)$$

We define three statistical quantities  $(z_0, z_1, z_2) \equiv (\sum_n s_n, \frac{1}{2} \sum_n s_n \cos \varphi_n, \frac{1}{2} \sum_n s_n \sin \varphi_n)$  where  $z_0$  is a measure of the average receptor activity and where  $z_1$  and  $z_2$  measure the asymmetry in the receptor activity. Using the transformation  $(\alpha_1, \alpha_2) \equiv (p \cos \phi, p \sin \phi)$  we can write the system’s Hamiltonian as  $\mathcal{H}_N\{s_n\} = -\sum_n \varepsilon_n s_n = -\alpha_0 z_0 - (\alpha_1 z_1 + \alpha_2 z_2)/2$  and compute its logarithm partition function as follows,

$$\begin{aligned} \ln \mathcal{Q}_N &= \ln \prod_{n=1}^N (e^{\varepsilon_n} + e^{-\varepsilon_n}) = \sum_{n=1}^N \ln [2 \cosh(\alpha_0 + h_n)] \\ &= N \ln(2 \cosh \alpha_0) + \frac{N p^2}{64 \cosh^2 \alpha_0} + \mathcal{O}(p^4), \end{aligned} \quad (2)$$

where in the last step the summand is expanded in powers of  $p$  and the sum is replaced by an integral over  $[0, 2\pi]$ .

The partition function contains all the thermodynamic information we need to infer the gradient parameters  $p$  and  $\phi$ , or alternatively, the transformed parameters  $\alpha_1$  and  $\alpha_2$ . Since  $p^2 = \alpha_1^2 + \alpha_2^2$ , we have by Eq. (2):

$$\mathbb{E}[z_{1,2}] = 2 \frac{\partial \ln \mathcal{Q}_N}{\partial \alpha_{1,2}} = \frac{\alpha_{1,2} N C_0 K_d}{4(C_0 + K_d)^2} + \mathcal{O}(p^3), \quad (3)$$

$$\text{Var}[z_{1,2}^2] = 4 \frac{\partial^2 \ln \mathcal{Q}_N}{\partial \alpha_{1,2}^2} = \frac{N C_0 K_d}{2(C_0 + K_d)^2} + \mathcal{O}(p^2). \quad (4)$$

In addition, one can check that  $\text{Cov}[z_1, z_2] = 0$ . Thus, for small  $p$ , the joint probability density of  $z_1$  and  $z_2$  is

$$f(z_{1,2} | \alpha_{1,2}) \approx \frac{1}{2\pi\sigma^2} \exp \left[ -\frac{(z_1 - \mu\alpha_1)^2 + (z_2 - \mu\alpha_2)^2}{2\sigma^2} \right],$$

with  $\mu \equiv N C_0 K_d / (4(C_0 + K_d)^2)$  and  $\sigma^2 = 2\mu$  [21]. It is easy to show that the *maximum likelihood estimator* (MLE) [22] of  $\alpha_{1,2}$  is  $\hat{\alpha}_{1,2} = z_{1,2} / \mu$ . As an orthogonal transformation, the MLE of  $p$  and  $\phi$  are given by  $\hat{p} = \sqrt{\hat{\alpha}_1^2 + \hat{\alpha}_2^2} = \mu^{-1} \sqrt{z_1^2 + z_2^2}$  and  $\hat{\phi} = \arctan(\hat{\alpha}_2 / \hat{\alpha}_1) = \arctan(z_2 / z_1)$ , respectively. By the properties of MLE, both  $\hat{p}$  and  $\hat{\phi}$  tend to be unbiased and normal in the large  $N$  limit, i.e.,  $\hat{p} \xrightarrow{d} \mathcal{N}(p, \sigma_p^2)$  and  $\hat{\phi} \xrightarrow{d} \mathcal{N}(\phi, \sigma_\phi^2)$ , where “ $\xrightarrow{d}$ ” denotes convergence in distribution. The asymptotic variances in the gradient steepness and direction,  $\sigma_p^2$  and  $\sigma_\phi^2$ , can be derived from the Fisher information matrix [22], which is diagonal since  $p$  and  $\phi$  are indepen-

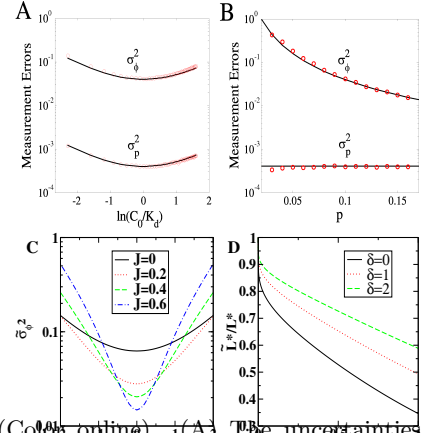


FIG. 2: (Color online). (A) The uncertainties  $\sigma_p^2$  and  $\sigma_\phi^2$  versus  $\ln(C_0/K_d)$  ( $p = 10\%$ ,  $N = 80000$ ) and versus  $p$  ( $C_0 = K_d$ ,  $N = 80000$ ). The solid lines correspond to the approximate analytical expressions while the symbols are the result of 5000 independent Monte-Carlo realizations. (C)  $\sigma_\phi^2$  as a function of  $\ln(C_0/K_d)$  for different values of  $J$ . (D) The critical cell size below which spatial gradient sensing is ineffective, normalized by the critical cell size in the absence of cooperativity, as a function of the cooperativity strength. In C and D, we have chosen  $N = 80000$  and  $p = 8\%$ .

dent. Thus,

$$\sigma_p^2 = 1/\mathbb{E}[(\partial_p \ln f)^2] = \frac{\sigma^2}{\mu^2} = \frac{2}{\mu} = \frac{8(C_0 + K_d)^2}{N K_d C_0}, \quad (5)$$

$$\sigma_\phi^2 = 1/\mathbb{E}[(\partial_\phi \ln f)^2] = \frac{\sigma^2}{\mu^2 p^2} = \frac{8(C_0 + K_d)^2}{N p^2 K_d C_0}. \quad (6)$$

and thus  $\sigma_\phi^2 = \sigma_p^2 / p^2$ . According to the Cramér-Rao inequality,  $\sigma_p^2$  and  $\sigma_\phi^2$  set the lowest uncertainties of gradient measurements from an instantaneous sampling of the receptor states [22]. The approximation for both variances is plotted in Fig. 2 as a function of the two parameters characterizing the gradient: the background concentration  $C_0$  (Fig. 2A) and the gradient steepness  $p$  (Fig. 2B). We have also performed Monte-Carlo simulations in which 80000 receptors are uniformly distributed along the circular cell membrane. Computing our statistical quantities for 5000 independent realizations, we determined the measurement errors and have plotted them as symbols in Fig. 2. The analytical results agree well with the numerically obtained values. From Fig. 2, we can see that the variances reach a minimum for  $C_0 = K_d$  while only the error in the gradient direction depends on the steepness of the gradient ( $\sigma_\phi^2 \sim p^{-2}$ ). Thus, since  $p = p_0 L$  (with  $p_0 = \frac{1}{C_0} \frac{dC}{dr}$ ) increases with the cell’s size, larger cells are able to sense the gradient direction with higher accuracy.

The above results are derived from a single snapshot of the system. If the cell integrates receptor signals over some time interval  $\mathcal{T}$ , then averaging over multiple measurements can appreciably reduce the errors of gradient sensing. However, the capacity of such averaging is limited by the expected time it takes for every independent

measurement. As shown in [8, 14], the time to complete a single measurement is roughly twice the system's correlation time  $\tau$  resulting from the diffusion and binding of ligand molecules, leading to a reduction of the variance:  $\sigma_{p,\tau}^2 = \frac{2\tau}{T}\sigma_p^2$ . The correlation time is given by  $\tau = \tau_{\text{rec}} + \tau_{\text{diff}}$ , where  $\tau_{\text{rec}} = 1/(k_- + C_0 k_+)$  is the timescale of receptor-ligand reaction and  $\tau_{\text{diff}}$  describes the diffusive transport time of ligands. Let  $\eta \equiv \tau_{\text{diff}}/\tau_{\text{rec}}$ , then the measurement is reaction-limited if  $\eta \ll 1$  and diffusion-limited if  $\eta \gg 1$ . From the above arguments we find that averaging signals over  $\mathcal{T}$  yields a lower uncertainty of the gradient estimate,

$$\sigma_{p,\tau}^2 \simeq \frac{2\tau}{T}\sigma_p^2 = \frac{4\tau_{\text{rec}}(1+\eta)}{\mu T} = \frac{16(1+\eta)}{NTk_-} \left(1 + \frac{K_d}{C_0}\right) \quad (7)$$

For small background concentrations ( $C_0 \ll K_d$ ),  $\tau_{\text{diff}} = N/(2\pi LDK_d)$  where  $D$  denotes the ligand diffusion coefficient [12, 14, 23], and the uncertainty reduces to  $\sigma_{p,\tau}^2 \simeq 16/(NTC_0 k_+) + 8/(\pi TDL C_0)$ . This expression contains two terms: the first one is determined by the chemical kinetics, and the second one, up to a geometric constant, is exactly the Berg-Purcell limit [12] or the result recently derived in [16]. We can derive similar results for the direction inference, since  $\sigma_{\phi,\tau}^2 = \sigma_{p,\tau}^2/p^2$ . For typical eukaryotic cells, it has been estimated [14, 23] that  $\eta \ll 1$ , which implies  $\sigma_{\phi,\tau}^2 \simeq 16(1 + K_d/C_0)/(Np^2 \mathcal{T} k_-) \sim 1/(Np^2)$ . We can relate the uncertainty in the direction measurement to the cell's size  $L$ . Assuming that the number of receptors in our model scales with the cell size as  $N = N_0 L^\delta$  with  $0 \leq \delta \leq 2$ , we find  $\sigma_{\phi,\tau}^2 \sim L^{-(2+\delta)}$ . For comparison, the Berg-Purcell analysis considered only an average concentration measurement and scales as  $\sigma_{c,\tau}^2 \sim L^{-1}$  [12]. Not surprisingly, our results indicate that spatial directional sensing can be more sensitive to the cell's size.

Our analysis above, which extends beyond the Berg-Purcell framework by providing a direct calculation of the directional sensing limit  $\sigma_{\phi,\tau}^2$ , was carried out for *independent* receptors, as is assumed to be the case for most eukaryotic cells that have been studied to date. We now ask, what if there is receptor cooperativity as has been found in many bacterial cells [24–26]? Intuitively, short-range interactions make it possible for receptors to collectively respond and thus sharpens the asymmetry of receptor signals. It is natural to speculate that such enhanced sensitivity may set new and lower limits for directional sensing. To incorporate potential receptor cooperativity, we extend our model to include a nearest-neighbor interaction  $J$  (again, in units of the thermal energy  $k_B T$ ). Now, the activity of a receptor, again represented by  $\{s_n = \pm 1\}_{n=1}^N$ , is determined not only by the local chemical concentration but also by the states of its neighboring receptors. This means that an unbound receptor is not necessarily inactive, as it may have been affected by active, nearby receptors.

Because the local concentration is identical for nearest-neighbor sites (i.e.,  $\varepsilon_n = \varepsilon_{n\pm 1}$ ), the Hamiltonian of our Ising chain can be written in a symmetric form:  $\tilde{\mathcal{H}}_N\{s_n\} = -\sum_{n=1}^N [Js_n s_{n+1} + \varepsilon_n(s_n + s_{n+1})/2]$ , with

the boundary condition  $s_{N+1} = s_1$ . The corresponding partition function is  $\tilde{\mathcal{Q}}_N = \sum_{s_1} \dots \sum_{s_N} e^{-(H_0 + H_1)}$ , where  $H_0 \equiv -\sum_n [Js_n s_{n+1} + \alpha_0(s_n + s_{n+1})/2]$  represents the Hamiltonian of an isotropic reference system and where  $H_1 \equiv -\sum_n s_n h_n = -\frac{p}{4} \sum_n s_n \cos(\varphi_n - \phi)$  results from the spatial heterogeneity of the concentration. For small  $p$ , one can view  $H_1$  as a perturbation to  $H_0$ . The partition function of the reference system,  $\tilde{\mathcal{Q}}_N^{(0)}$ , is exactly solvable [27], e.g., using the transfer matrix  $\mathcal{P} \equiv \begin{pmatrix} e^{J+\alpha_0} & e^{-J} \\ e^{-J} & e^{J-\alpha_0} \end{pmatrix}$  such that

$$\tilde{\mathcal{Q}}_N^{(0)} = \sum_{s_1} \dots \sum_{s_N} e^{-H_0} = \text{Tr}(\mathcal{P}^N) = \lambda_+^N + \lambda_-^N, \quad (8)$$

with  $\lambda_{\pm} = e^J \cosh \alpha_0 \pm \sqrt{e^{-2J} + e^{2J} \sinh^2 \alpha_0}$  being the eigenvalues of  $\mathcal{P}$ . Thus,  $\ln \tilde{\mathcal{Q}}_N^{(0)} \rightarrow N \ln \lambda_+$  for large  $N$ . The statistical perturbation theory inspires us to write  $\tilde{\mathcal{Q}}_N = \tilde{\mathcal{Q}}_N^{(0)} \sum_{s_1} \dots \sum_{s_N} e^{-H_0} e^{-H_1} / \tilde{\mathcal{Q}}_N^{(0)} = \tilde{\mathcal{Q}}_N^{(0)} \langle e^{-H_1} \rangle \simeq \lambda_+^N [1 + \frac{p}{4} \sum_n \langle s_n \rangle \cos \theta_n + \frac{p^2}{32} \sum_{n,m} \langle s_n s_m \rangle \cos \theta_n \cos \theta_m]$ . Here, we denote  $\theta_n \equiv \varphi_n - \phi$  for short and use  $\langle \cdot \rangle$  to represent the expectation over the reference system. Due to isotropy,  $\langle s_n \rangle$  is independent of its location (index  $n$ ) and hence  $\sum_n \langle s_n \rangle \cos \theta_n = \langle s_n \rangle \sum_n \cos \theta_n = 0$ . We further calculate that  $\sum_{n,m} \langle s_n s_m \rangle \cos \theta_n \cos \theta_m = \frac{N}{2}(1 + 2\xi)/(1 + e^{4J} \sinh^2 \alpha_0)$ , [28], where  $\xi \equiv [\ln(\lambda_+/\lambda_-)]^{-1}$  defines the correlation length of the classic Ising chain [27]. Finally, the log-partition function of our model is

$$\ln \tilde{\mathcal{Q}}_N \simeq N \ln \lambda_+ + \frac{Np^2(1 + 2\xi)}{64(1 + e^{4J} \sinh^2 \alpha_0)} + \mathcal{O}(p^3), \quad (9)$$

which reduces to Eq. (2) as  $J \rightarrow 0$ .

Now we rewrite  $\tilde{\mathcal{H}}_N = -J \sum_n s_n s_{n+1} - \alpha_0 z_0 - (\alpha_1 z_1 + \alpha_2 z_2)/2$ , with the same notations for  $\alpha_i$  and  $z_i$ ,  $i = 0, 1, 2$ . As has been demonstrated before, the MLE of  $\alpha_1$  and  $\alpha_2$  can be found from the joint Gaussian distribution of  $z_1$  and  $z_2$ , except now we have to replace  $\mu$  by  $\tilde{\mu} \equiv \frac{1}{16}N(1 + 2\xi)/(1 + e^{4J} \sinh^2 \alpha_0)$ . So the MLE of  $p$  and  $\phi$  are given by  $\tilde{p} = \tilde{\mu}^{-1} \sqrt{z_1^2 + z_2^2} \xrightarrow{d} \mathcal{N}(p, \tilde{\sigma}_p^2)$  and  $\tilde{\phi} = \arctan(z_2/z_1) \xrightarrow{d} \mathcal{N}(\phi, \tilde{\sigma}_\phi^2)$ . Similar to Eq. (5-6), their variances are  $\tilde{\sigma}_p^2 = 2/\tilde{\mu}$  and  $\tilde{\sigma}_\phi^2 = \tilde{\sigma}_p^2/p^2 = 2/(\tilde{\mu}p^2)$  [29]. We plot  $\tilde{\sigma}_\phi^2$  as a function of  $\ln(C_0/K_d)$  for different values of  $J$  in Fig. 2C. Regardless of the receptor coupling strength, this error is minimal at  $C_0 = K_d$  (or  $\alpha_0 = 0$ ) where the correlation length is  $\xi = 1/\ln(\coth J) \simeq \frac{1}{2}e^{2J}$  and  $\tilde{\sigma}_\phi^2 \simeq 32/[Np^2(1 + e^{2J})] = \sigma_\phi^2/(1 + e^{2J})$ .

Receptor cooperativity may help a smaller cell of diameter  $\tilde{L}$  achieve the same level of accuracy as a larger cell of diameter  $L$  with independent receptors, i.e.,  $\tilde{\sigma}_\phi^2(\tilde{L}) = \sigma_\phi^2(L)$ . By our previous scaling assumption, the receptor number of the smaller cell is  $\tilde{N} = N(\tilde{L}/L)^\delta$ . If  $L^*$  denotes a critical cell length below which spatial sensing is infeasible with non-cooperative receptors, then adding cooperativity will push the critical cell size,  $\tilde{L}^*$ , lower by

a factor of  $(1 + 2\xi)^{-1/(2+\delta)} \simeq L(1 + e^{2J})^{-1/(2+\delta)}$ . This is shown in Fig. 2D where we have plotted  $\tilde{L}^*/L^*$  as a function of  $J$  for three values of the scaling factor  $\delta$ . As a specific example, we take  $L^* = 8\mu\text{m}$  which corresponds to the typical size of a *Dictyostelium* amoeba. Then, we see that for a cooperativity of  $J = 0.5$  the new critical size becomes  $\tilde{L}^* \sim 4 - 6\mu\text{m}$ , comparable to the size of many bacterial cells. It is worth remarking that although receptor interaction improves the precision of gradient sensing for  $C_0$  close to  $K_d$ , it enlarges the errors when  $C_0$  is far away from  $K_d$  (Fig. 2C). In other words, the improved accuracy near  $K_d$  is at the cost of the sensitivity range of background concentrations. Such a tradeoff could be a limiting factor for the introduction of coupling into the spatial sensing mechanism.

It is commonly believed that prokaryotic cells such as *E. coli* are too small to perform spatial sensing of chemical gradients. However, recent experimental observations show that at least one type of vibrioid bacteria (typical size  $2 \times 6 \mu\text{m}$ ) are able to spatially sense gradients along distances as short as  $5 \mu\text{m}$  [19]. Our results allow for the possibility that smaller organisms employ a spatial sensing strategy with the aid of receptor cooperativity. As spatial sensing is argued to be superior to temporal sensing for fast swimming bacteria [19, 30], this possibility is of significant theoretical interest and remains a challenge for future empirical studies.

We thank W. Loomis, B. Li, R.J. Williams, J. Wolf, and M. Skoge for valuable discussions. This work was supported by NIH Grant P01 GM078586.

- 
- [1] C.A. Parent and P.N. Devreotes, *Science*. **284**, 765 (1999).
  - [2] P.J.V. Haastert and P.N. Devreotes, *Nat. Rev. Mol. Cell Biol.* **5**, 626 (2004).
  - [3] R.M. Macnab and D.E. Koshland, *Proc. Natl. Acad. Sci. U.S.A.* **69**, 2509 (1972).
  - [4] J.E. Segall *et al.*, *Proc. Natl. Acad. Sci. U.S.A.* **83**, 8987 (1986).
  - [5] V. Sourjik and H.C. Berg, *Proc. Natl. Acad. Sci. U.S.A.* **99**, 123 (2002).
  - [6] D. Bray *et al.*, *Nature*, **393**, 85 (1998).
  - [7] L. Song, *et al.*, *Eur. J. Cell Biol.* **85**, 981 (2006).
  - [8] P.J.V. Haastert and M. Postma, *Biophys. J.* **93**, 1787 (2007).
  - [9] D. Fuller *et al.*, *Proc. Natl. Acad. Sci. U.S.A.* (to be published).
  - [10] M. Ueda *et al.*, *Science*, **294**, 864 (2001).
  - [11] M. Ueda and T. Shibata, *Biophys. J.* **93**, 11 (2007).
  - [12] H.C. Berg and E.M. Purcell, *Biophys. J.* **20**, 193 (1977).
  - [13] W. Bialek and S. Setayeshgar, *Proc. Natl. Acad. Sci. U.S.A.* **102**, 10040 (2005).
  - [14] K. Wang *et al.*, *Phys. Rev. E* **75**, 061905 (2007).
  - [15] W. Bialek and S. Setayeshgar, *Phys. Rev. Lett.* **100**, 258101 (2008).
  - [16] R.G. Endres and N.S. Wingreen, *Proc. Natl. Acad. Sci. U.S.A.* **105**, 15749 (2008).
  - [17] R.G. Endres and N.S. Wingreen, *Phys. Rev. Lett.* **103**, 158101 (2009).
  - [18] W.-J. Rappel and H. Levine, *Phys. Rev. Lett.* **100**, 228101 (2008); W.-J. Rappel and H. Levine, *Proc. Natl. Acad. Sci. U.S.A.* **105**, 19270 (2008).
  - [19] R. Thar and M. K hl, *Proc. Natl. Acad. Sci. U.S.A.* **100**, 5748 (2003).
  - [20] This assumption is for analytical convenience and can be relaxed numerically. Our theoretical results work well even if the receptors are assumed to be uniformly distributed at random on the cell surface.
  - [21] B. Hu *et al.*, *Phys. Rev. E* **81**, 031906 (2010).
  - [22] S.M. Kay, *Fundamentals of Statistical Signal Processing: Estimation Theory* (Prentice Hall PTR, Upper Saddle River, NJ, 1993), Vol. 1, Chap. 3.
  - [23] D.A. Lauffenburger and J.J. Linderman, *Receptors: Models for Binding, Trafficking, and Signaling* (Oxford University Press, New York, 1993), Chap. 4.
  - [24] Y. Shi and T. Duke, *Phys. Rev. E* **58**, 6399 (1998).
  - [25] B.A. Mello and Y. Tu, *Proc. Natl. Acad. Sci. U.S.A.* **100**, 8223 (2003); B.A. Mello and Y. Tu, *ibid.* **102**, 17354 (2005); B.A. Mello *et al.*, *Biophys. J.* **87**, 1578 (2004).
  - [26] J.E. Keymer *et al.*, *Proc. Natl. Acad. Sci. U.S.A.* **103**, 1786 (2006); M.L. Skoge, R.G. Endres, and N.S. Wingreen, *Biophys. J.* **90**, 4317 (2006).
  - [27] R.J. Baxter, *Exactly Solved Models in Statistical Mechanics* (Academic, London, 1982), Chap. 2.
  - [28] For the classic Ising chain, the spin-spin correlation is  $\langle s_n s_m \rangle = \cos^2 2\omega + \gamma^{|n-m|} \sin^2 2\omega$ , where  $\gamma = \lambda_-/\lambda_+$  and  $\omega$  is defined by the equation  $\cot 2\omega = e^{2J} \sinh \alpha_0$  for  $0 < \omega < \pi/2$  [27]. Thanks to  $\sum_n \sum_m \cos^2 2\omega \cos \theta_n \cos \theta_m = \cos^2 2\omega \sum_n \cos \theta_n \sum_m \cos \theta_m = 0$ , we only need calculate  $\sum_n \sum_m \cos \theta_n \cos \theta_m \gamma^{|n-m|} = \sum_n \cos \theta_n \sum_m \cos[(\theta_m - \theta_n) + \theta_n] \gamma^{|n-m|} = \sum_n \cos^2 \theta_n \sum_m \cos(\theta_m - \theta_n) \gamma^{|n-m|} - \sum_n \cos \theta_n \sin \theta_n \sum_m \sin(\theta_m - \theta_n) \gamma^{|n-m|}$ . The second term vanishes since we have  $\sum_m \sin(\theta_m - \theta_n) \gamma^{|n-m|} = \sum_{j=-N/2}^{N/2} \sin(2\pi j/N) \gamma^{|j|} = 0$ , while the first term above is identical to  $\sum_n \cos^2 \theta_n \sum_{j=-N/2}^{N/2} \cos(2\pi j/N) \gamma^{|j|} = \sum_n \cos^2 \theta_n \left[ 1 + 2 \sum_{j=1}^{N/2} \cos(2\pi j/N) \gamma^j \right]$ . For large  $N$ , we have that  $\sum_n \cos^2 \theta_n \simeq N/2$  and  $\sum_{j=1}^{N/2} \cos(2\pi j/N) \gamma^j \simeq \frac{N}{2\pi} \int_0^\pi \cos(x) \exp\left(\frac{xN}{2\pi} \ln \gamma\right) dx \xrightarrow{N \rightarrow \infty} -1/\ln \gamma \equiv \xi$ . Thus,  $\sum_{n,m} \langle s_n s_m \rangle \cos \theta_n \cos \theta_m = \frac{N}{2} (1 + 2\xi) \sin^2 2\omega = \frac{N}{2} (1 + 2\xi)/(\cot^2 2\omega + 1) = \frac{N}{2} (1 + 2\xi)/(1 + e^{4J} \sinh^2 \alpha_0)$ .
  - [29] As long as we are not near any phase transition point, the measurement decorrelation time will remain dominated by the processes of diffusion and binding/unbinding of ligand molecules [15]. Thus, averaging signals over  $\mathcal{T}$  will give  $\tilde{\sigma}_{p,\mathcal{T}}^2 \simeq 4\tau_{\text{rec}}(1 + \eta)/(\tilde{\mu}\mathcal{T})$  and  $\tilde{\sigma}_{\phi,\mathcal{T}}^2 = \tilde{\sigma}_{p,\mathcal{T}}^2/p^2$ .
  - [30] D.B. Dusenbery, *Biophys. J.* **74**, 2272 (1998).